AJNR

This information is current as of August 12, 2025.

Diagnostic Accuracy of Dynamic Contrast-Enhanced MR Imaging Using a Phase-Derived Vascular Input Function in the Preoperative Grading of Gliomas

T.B. Nguyen, G.O. Cron, J.F. Mercier, C. Foottit, C.H. Torres, S. Chakraborty, J. Woulfe, G.H. Jansen, J.M. Caudrelier, J. Sinclair, M.J. Hogan, R.E. Thornhill and I.G. Cameron

ORIGINAL
RESEARCH

T.B. Nguyen
G.O. Cron
J.F. Mercier
C. Foottit
C.H. Torres
S. Chakraborty
J. Woulfe
G.H. Jansen
J.M. Caudrelier
J. Sinclair
M.J. Hogan
R.E. Thornhill
I.G. Cameron

Diagnostic Accuracy of Dynamic Contrast-Enhanced MR Imaging Using a Phase-Derived Vascular Input Function in the Preoperative Grading of Gliomas

BACKGROUND AND PURPOSE: The accuracy of tumor plasma volume and K^{trans} estimates obtained with DCE MR imaging may have inaccuracies introduced by a poor estimation of the VIF. In this study, we evaluated the diagnostic accuracy of a novel technique by using a phase-derived VIF and "book-end" T1 measurements in the preoperative grading of patients with suspected gliomas.

MATERIALS AND METHODS: This prospective study included 46 patients with a new pathologically confirmed diagnosis of glioma. Both magnitude and phase images were acquired during DCE MR imaging for estimates of K^{trans}_φ and V_p_φ (calculated from a phase-derived VIF and bookend T1 measurements) as well as K^{trans}_SI and V_p_SI (calculated from a magnitude-derived VIF without T1 measurements).

RESULTS: Median K^{trans}_φ values were 0.0041 minutes^{-1} (95% CI, 0.00062–0.033), 0.031 minutes^{-1} (0.011–0.150), and 0.088 minutes^{-1} (0.069–0.110) for grade II, III, and IV gliomas, respectively ($P \leq$ .05 for each). Median V_p_φ values were 0.64 mL/100 g (0.06–1.40), 0.98 mL/100 g (0.34–2.20), and 2.16 mL/100 g (1.8–3.1) with $P =$ .15 between grade II and III gliomas and $P =$ .015 between grade III and IV gliomas. In differentiating low-grade from high-grade gliomas, AUCs for K^{trans}_φ, V_p_φ, K^{trans}_SI, and V_p_SI were 0.87 (0.73–1), 0.84 (0.69–0.98), 0.81 (0.59–1), and 0.84 (0.66–0.91). The differences between the AUCs were not statistically significant.

CONCLUSIONS: K^{trans}_φ and V_p_φ are parameters that can help in differentiating low-grade from high-grade gliomas.

ABBREVIATIONS: AUC = area under the receiver operating characteristic curve; $C_T(t)$ = tissue contrast concentration curve with time; CI = confidence interval; CV = coefficient of variation; DCE = dynamic contrast-enhanced; K^{trans}_φ = volume transfer coefficient obtained from phase-derived vascular input function; K^{trans}_SI = volume transfer coefficient obtained from magnitude-derived vascular input function; NPV = negative predictive value; PPV = positive predictive value; R_1 = rate of longitudinal relaxation; R_2^* = observed rate of transverse relaxation; ROC = receiver operating characteristic analysis; T_1 = longitudinal relaxation time; V_p_SI = plasma volume obtained from magnitude-derived vascular input function; VIF = vascular input function; V_p_φ = plasma volume obtained from phase-derived vascular input function

Contrast-enhanced anatomic MR imaging is not always accurate in differentiating high-grade gliomas from low-grade gliomas.[1] The presence of contrast enhancement is more common in higher grade gliomas but is not infrequently found in low-grade tumors. Physiologic imaging such as perfusion MR imaging has been used recently to evaluate angiogenesis, which is important for both the growth and metastasis of malignant tumors.[2] The 2 most common MR perfusion techniques used in clinical practice are dynamic susceptibility-weighted contrast-enhanced imaging and DCE imaging.[3] Following an intravenous injection of a Gd-based contrast agent, dynamic susceptibility-weighted contrast-enhanced imaging measures the change in R_2^* during the first pass of the bolus, while DCE imaging measures the changes in R_1 during both the first pass and washout phases.

While DCE perfusion might be more accurate than dynamic susceptibility-weighted contrast-enhanced in the measurement of parameters such as cerebral blood volume and permeability index, DCE usually requires more complex data acquisition and analysis. First, determination of T1 values in brain tissue before contrast injection is now usually done for calculation of $C_T(t)$ from changes in R_1 following bolus injection.[4] Additional measurements of T1 values following contrast injection, "bookend" measurements, have also been performed to improve the accuracy of DCE parameters.[5] Second, an accurate VIF is needed but is difficult to obtain because the relationship between MR signal intensity and absolute contrast concentration is not always linear and might be compromised by inflow.[6,7] Recently, several authors have proposed the use of phase information to derive the VIF.[8,9] It is known that if a vessel is approximately parallel to the magnetic field, changes in gadolinium-based contrast agent concentration vary linearly with phase
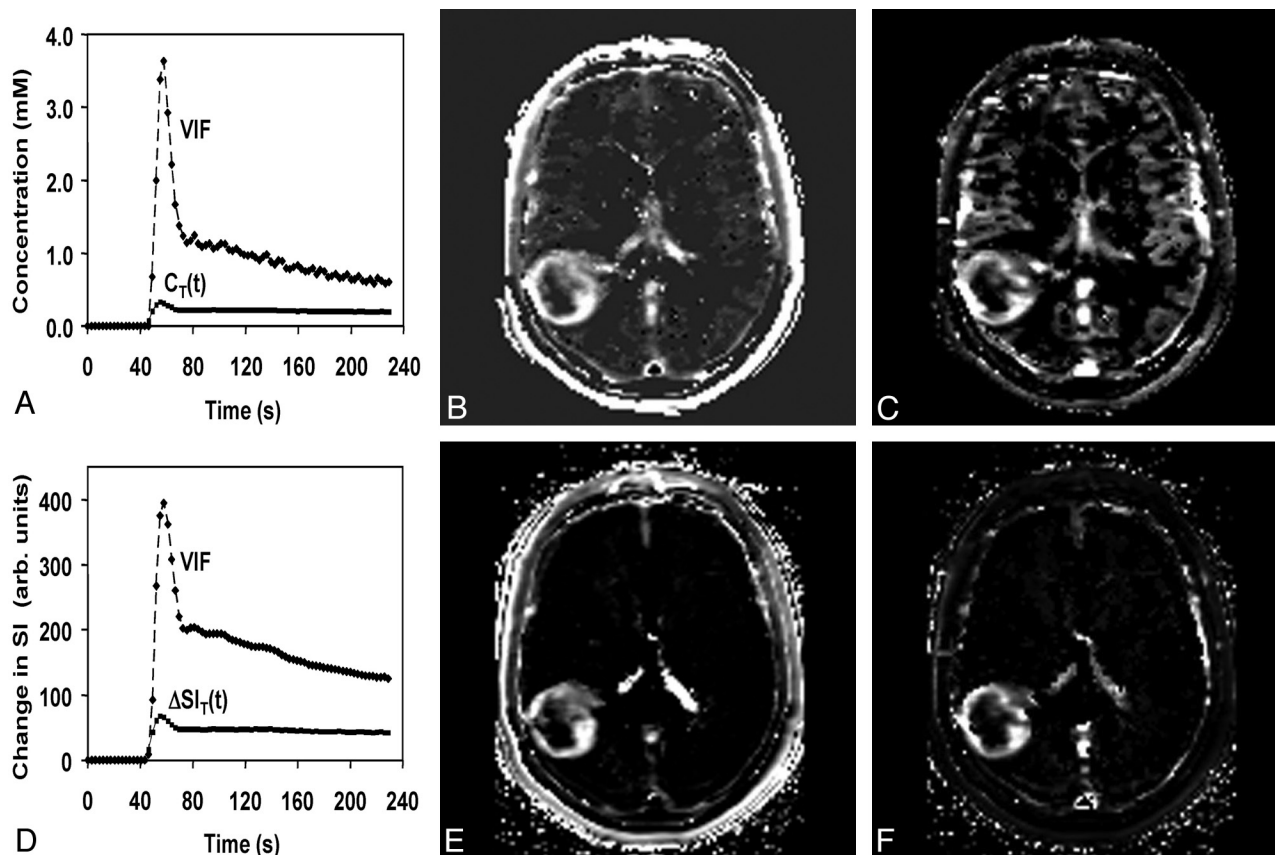
Fig 1. *A*, Phase-derived VIF and tumor $C_T(t)$ from a patient with confirmed grade IV glioma obtained at 3T. *B* and *C*, K^{trans}_φ (*B*) and V_p_φ (*C*) maps. *D*, Magnitude-derived VIF and tumor signal-intensity changes from the same patient for comparison. *E* and *F*, K^{trans}_SI (*E*) and V_p_SI (*F*) maps. Maximal K^{trans}_φ and V_p_φ values in tumor are 0.099 minutes^{-1} and 5.7 mL/100 g compared with 0.15 minutes^{-1} and 18 mL/100 g for K^{trans}_SI and V_p_SI.

changes.[10] Because phase images can be acquired at the same time as magnitude images, no additional imaging is required.

In this study, we evaluated the diagnostic accuracy of DCE MR imaging parameters by using phase-derived VIF and bookend T1 measurements in the preoperative grading of patients with suspected gliomas. We compared this technique with a simpler pharmacokinetic analysis by using magnitude-derived VIF without T1 mapping.

Materials and Methods
Subjects

All examinations were conducted in accordance with the guidelines of our institution for human research, and written informed consent was obtained from all participating subjects. All adult patients presenting at the Ottawa Hospital with a newly diagnosed brain lesion compatible with a glioma between December 2008 and March 2010 were included in this prospective study. We set the following exclusion criteria: pregnancy, renal failure, and a known history of allergy to gadolinium-based MR imaging contrast agent. Following the MR imaging examination, patients underwent surgery with biopsy or surgical resection of the lesion. The average time interval between the MR imaging examination and surgery was 12.5 days. Histopathologic diagnosis was provided by an experienced neuropathologist (J.W., 12 years of experience, or G.H.J., 23 years of experience) by using the World Health Organization classification.

MR Imaging Acquisition

All MR imaging data were acquired by using either a 1.5T (Symphony; Siemens, Erlangen, Germany) or a 3T clinical scanner (Trio, Siemens).

Anatomic imaging was performed by using standard sagittal T1-weighted and axial T1-weighted pre- and post-DCE contrast injection; and axial FLAIR, axial T2, and coronal T1 post-DCE contrast injection.

At 1.5T, DCE MR imaging was performed by using a 2D fast low-angle shot pulse sequence (5 axial sections, TR = 45 ms, TE = 2.1, 5.5 ms, flip angle = 90°, matrix = 96 × 128, FOV = 17 × 23 cm^2, section thickness = 5 mm, Δt = 2.2 seconds). 2D fast low-angle shot was used for dynamic imaging on the 1.5T scanner because of hardware limitations. The desired temporal resolution ($\Delta t < 3$ seconds) was only achievable with the 2D sequences. At 3T, a 3D fast low-angle shot sequence was used (18 axial sections, TR = 6.5 ms, TE = 1.7, 3.9 ms, flip angle = 30°, matrix = 96 × 128, FOV = 23 cm^2, section thickness = 5 mm, Δt = 2.9 seconds). The 2D and 3D fast low-angle shot sequences generated phase images in addition to the standard magnitude images. Both before and after the DCE MR imaging, a series of gradient-echo images was acquired, which enabled the calculation of T1 maps. 3D fast low-angle shot images (TR = 50 ms, TE = 2.2 ms, flip angle = 10°, 20°, 40°, 70°) were obtained at 1.5T, and 3D volumetric interpolated breathhold examination images (TR = 20 ms, TE = 1.2 ms, flip angle = 4°, 25°) were used at 3T. 3D sequences were used on both scanners for T1 mapping, to minimize section profile effects. For T1 mapping on the 3T scanner, volumetric interpolated breathhold examination was used instead of fast low-angle shot, though the contrast mechanisms of these 2 sequences are very similar (T1-weighted spoiled gradient-echo). A shorter TR and fewer flip angles were used for T1 mapping at 3T to reduce scanning time.

Table 1: Median values of the maximal perfusion parameters and coefficient of variation for different grades of gliomas using a 2D gradient-recalled echo sequence on a 1.5T MR imaging scanner

	No.	K^{trans}_φ (min^{-1}) (95% CI)	CV (%)	K^{trans}_SI (min^{-1}) (95% CI)	CV (%)	V_p_φ (mL/100 g) (95% CI)	CV (%)	V_p_SI (ml/100 g) (95% CI)	CV (%)
Grade 2	8	0.0086 (0.0010–0.047)	153	0.0032 (0.00056–0.17)	210	0.66 (0.091–1.55)	91	1.35 (0.22–6.9)	143
Grade 3	4	0.020	142	0.0052	191	1.37	105	2.8	114
		Not defined		Not defined		Not defined		Not defined	
Grade 4	19	0.10 (0.072–0.13)	46	0.13 (0.073–0.23)	85	2.0 (1.7–3.1)	78	8.8 (5.3–14)	76

Table 2: Median values of the maximal perfusion parameters and coefficient of variation for different grades of gliomas using a 3D gradient-recalled echo sequence on a 3T MR scanner

	No.	K^{trans}_φ (min^{-1}) (95% CI)	CV (%)	K^{trans}_SI (min^{-1}) (95% CI)	CV (%)	V_p_φ (mL/100 g) (95% CI)	CV (%)	V_p_SI (mL/100 g) (95% CI)	CV (%)
Grade 2	1	0		0		0		0	
		Not defined		Not defined		Not defined		Not defined	
Grade 3	5	0.032	122	0.026	131	0.98	54	3.9	57
		Not defined		Not defined		Not defined		Not defined	
Grade 4	9	0.069 (0.047–0.096)	45	0.15 (0.082–0.31)	72	2.4 (1.3–5.6)	59	12.5 (5.5–25)	70

This was possible due to the additional signal intensity–to-noise ratio available on that machine.

Gadopentetate dimeglumine (Magnevist; Bayer Schering, Berlin, Germany) was injected at 0.1 mmol/kg and 4 mL/s, beginning 40 seconds after the start of the scan. The duration of the DCE sequence was 220 seconds.

Pharmacokinetic Modeling

Phase-Derived VIF with Bookend T1 Correction. Voxel wise maps of $C_T(t)$ were calculated in 2 steps. First, the double echo was used to extrapolate all magnitude signals to TE = 0 ms, thereby reducing T2* effects. Second, the pre- and post-DCE T1 maps were combined with the extrapolated tissue signal-intensity-versus-time curve by using standard signal-intensity equations to compute $C_T(t)$. The VIF was calculated from the superior sagittal sinus by measuring the change in phase as a function of time, taking into account the angle of each vessel segment relative to the main magnetic field. This step was performed off-line by using in-house software written in IDL (ITT Visual Information Solutions, Boulder, Colorado) and is described in a previous article.[8] Voxel-by-voxel estimates of V_p_φ and K^{trans}_φ were determined by using a kinetic model analysis from the nordicICE software (Version 2; NordicNeuroLab, Bergen, Norway) as described in the Appendix. Representative parametric maps of V_p_φ and K^{trans}_φ are shown in Fig 1B, -C.

Magnitude-Derived VIF with No T1 Correction. DCE magnitude images were processed directly in Nordic ICE to generate maps of V_p_SI and K^{trans}_SI as described in the Appendix (Fig 1D, -E).

Image Interpretation

Two neuroradiologists, blinded to the pathologic diagnosis (C.H.T. and S.C., with 3 and 5 years of experience, respectively) interpreted the structural images. Based on standard radiologic criteria of contrast enhancement, central necrosis, and vasogenic edema, each radiologist graded the glioma from 1 to 4. A senior radiology resident (J.F.M., third-year radiology resident) traced 4 ROIs of 25 mm^2 in the solid part of the tumor. The maximum value of the 4 mean values from the ROIs was obtained for K^{trans} and V_p for each pharmacokinetic approach. All ROIs were verified by a neuroradiologist (T.B.N., 10 years of experience) to ensure that inadvertent placement on an adjacent vessel was avoided.

Statistical Analysis

All data were analyzed by using MedCalc for Windows, Version 11.5 (MedCalc Software, Mariakerke, Belgium). There were 6 components to the statistical analysis: 1) calculation of sensitivity and specificity for each reader by using anatomic MR imaging to grade gliomas, 2) assessment of inter-reader reliability by using the κ statistic. 3) tests for difference in maximum V_p and K^{trans} values according to grade by using the Mann-Whitney U test, 4) tests for difference in maximum V_p and K^{trans} values according to the MR imaging acquisition method (2D-versus-3D fast low-angle shot) by using the Mann-Whitney U test, 5) ROC analysis for V_p and K^{trans} in grading gliomas by using each method, and 6) Bland-Altman analysis of within-subject reproducibility of V_p and K^{trans} values by using both methods and testing for difference between values by using a paired Wilcoxon test.

Results

Participants

During the study period, a total of 60 patients presented with a newly diagnosed brain lesion and had DCE MR imaging. Six patients did not have any surgery, 6 patients had a pathologic diagnosis other than glioma following surgery (1 normal brain tissue, 4 metastasis, 1 supratentorial ependymoma grade III), and 2 patients had missing data from MR perfusion imaging. Forty-six patients with a newly pathologically proved diagnosis of glioma were included in the analysis (9 grade II, 9 grade III, 28 grade IV) with 42 astrocytomas, 3 oligoastrocytomas, and 1 oligodendroglioma.

Accuracy of Conventional Imaging for Distinguishing Low-Grade from High-Grade Gliomas

In distinguishing low-grade (grade II) from high-grade gliomas (grades III and IV), reader 1 had a sensitivity of 97% and a specificity of 67% (PPV = 92%, NPV = 86%), while reader 2 achieved a sensitivity of 95% and a specificity of 67% (PPV = 92%, NPV = 75%). There was substantial agreement between the 2 readers ($\kappa = 0.76$, 95% CI, 0.50–1.0).

V_p and K^{trans} Values According to Glioma Grades

The median K^{trans} and V_p values for each glioma grade and for each MR imaging scanner are summarized in Tables 1–3 and

Table 3: Median values of the maximal perfusion parameters and coefficient of variation for different grades of gliomas combining 2D and 3D acquisition methods

	No.	K^{trans}_φ (min^{-1}) (95% CI)	CV (%)	K^{trans}_SI (min^{-1}) (95% CI)	CV (%)	V_p_φ (mL/100 g) (95% CI)	CV (%)	V_p_SI (mL/100 g) (95% CI)	CV (%)
Grade 2	9	0.0041 (0.00062–0.033)	165	0.0024 (0.00050–0.10)	224	0.64 (0.063–1.4)	103	1.12 (0.18–4.9)	155
Grade 2 excluding biopsy	6	0.0014 (0.00010–0.011)	144	0.0016 (0.00011–0.014)	156	0.15 (0.011–0.67)	107	0.81 (0.032–4.3)	133
Grade 3	9	0.031 (0.011–0.15)	122	0.0093 (0.0030–0.17)	172	0.98 (0.34–2.2)	92	3.7 (1.6–6.4)	86
Grade 3 excluding biopsy	7	0.031 (0.0083–0.19)	116	0.0093 (0.0017–0.29)	169	0.79 (0.26–2.9)	116	1.9 (1.0–8.6)	103
Grade 4	28	0.088 (0.069–0.11)	48	0.15 (0.093–0.21)	79	2.16 (1.8–3.1)	71	9.4 (5.8–14)	75
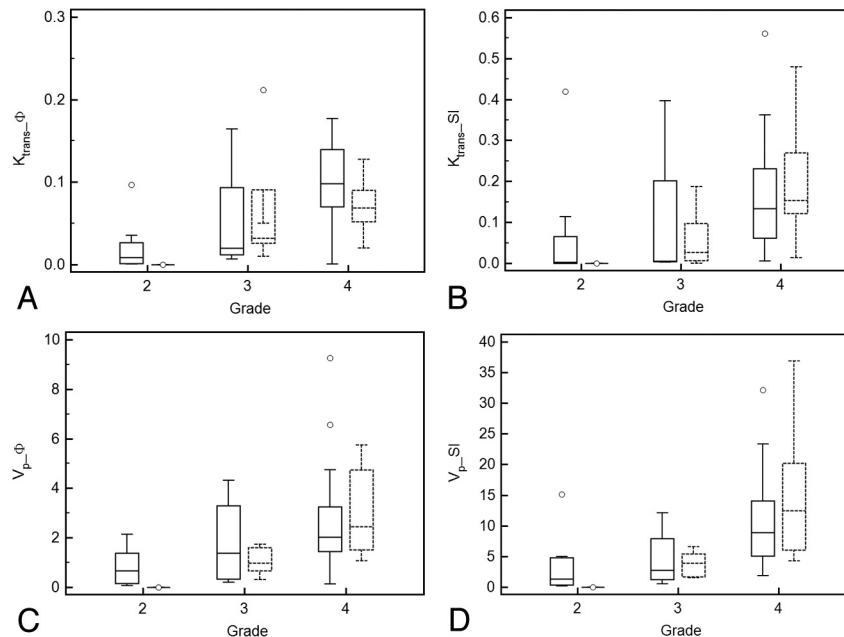
Fig 2. Boxplots showing ability of parameters K^{trans}_φ (*A*), K^{trans}_SI (*B*), V_p_φ (*C*), and V_p_SI (*D*) in differentiating various glioma grades for 2D (solid line) and 3D data (dashed line).

depicted graphically in Fig 2. There was a statistical difference in median K^{trans}_φ estimates between grades III and IV (Table 4). The difference in K^{trans}_φ between grade II and III gliomas is near statistical significance ($P = .050$) and becomes significant if we exclude patients who had a pathologic diagnosis from a stereotactic biopsy and not from a surgical resection ($P = .0047$).

Median V_p_φ values also increased with higher glioma grade. This difference was not statistically significant between grades II and III but was significant between grades III and IV (Table 4). The intersubject CVs were higher for low-grade gliomas than for high-grade gliomas.

With the magnitude-derived VIF approach, K^{trans}_SI values and V_p_SI values also differed on the basis of glioma grade (Tables 1–3) (Fig 2*C*, -*D*). There was a statistically significant difference found between grades III and IV but not between grades II and grade III (Table 4).

V_p and K^{trans} Values According to MR Imaging Acquisition Method (2D versus 3D)

In general, 3D acquisitions had lower intersubject CVs for both K^{trans} and V_p than 2D acquisitions. K^{trans}_φ values had lower intersubject CVs than K^{trans}_SI. V_p_φ values had lower CVs than V_p_SI except for grade III gliomas (Tables 1–3).

In the group of 9 patients with grade II gliomas, comparison between values obtained from the 2D fast low-angle shot sequence (1.5T scanner) and 3D fast low-angle shot sequence

(3T scanner) was not possible because only 1 patient was scanned on the 3T scanner (Tables 1 and 2). For patients with grade III, no statistical difference could be found between perfusion parameters obtained with 2D and 3D acquisition methods, but for grade IV gliomas, a near statistical difference was found with K^{trans}_φ ($P = .058$) (Table 4).

Accuracy of DCE MR Perfusion for Distinguishing Glioma Grades by using ROC

In distinguishing low-grade (II) from high-grade gliomas (III+IV), the highest AUC corresponded to K^{trans}_φ, followed by V_p_φ, V_p_SI, and K^{trans}_SI (Fig 3*A*, -*B*) (Table 5). However, the differences between the AUCs for K^{trans}_φ versus K^{trans}_SI and for V_p_φ versus V_p_SI did not reach statistical significance ($P = .18$ and $P = .87$, respectively). Using a threshold of K^{trans}_$\varphi > 0.018$ minutes^{-1}, we achieved a sensitivity of 89%

Table 4: The statistical significance (*P* Values) of differences in median perfusion parameter values for various grades of gliomas and imaging techniques

P Value	K^{trans}_φ	K^{trans}_SI	V_p_φ	V_p_SI
Grade II vs III	.050	.17	.15	.14
Grade II vs III excluding biopsy	.0047	.070	.051	.070
Grade III vs IV	.040	.014	.015	.0026
Grade III 2D vs 3D	.32	.62	.80	.80
Grade IV 2D vs 3D	.058	.50	.57	0.21

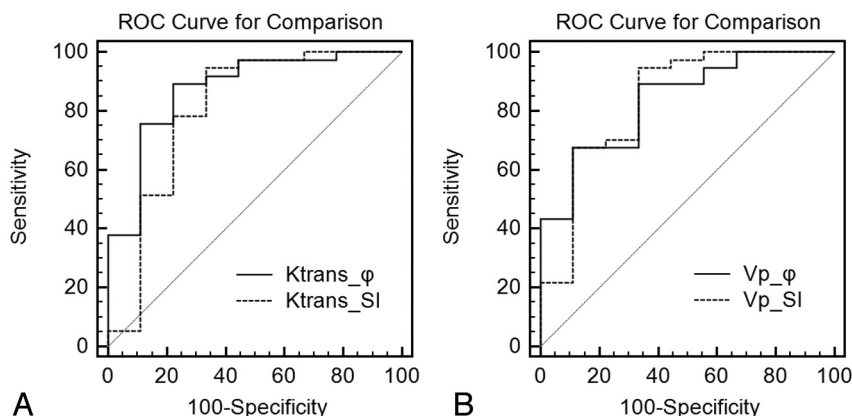**Fig 3.** *A*, ROC for comparison of maximal K^{trans}_φ and $K^{trans}\_$SI for differentiation of low-grade from high-grade gliomas. *B*, ROC for comparison of V_p_φ and $V_p\_$SI in differentiating low-grade and high-grade gliomas.

and a specificity of 75% (PPV = 94%, NPV = 62%). With a threshold of $V_p\_\varphi > 1.4$ mL/100 g, sensitivity was 68% and specificity was 89% (PPV = 96%, NPV = 40%).

In distinguishing grade III from grade IV gliomas, the AUCs associated with V_p_φ and $V_p\_$SI were slightly higher than those obtained for $K^{trans}\_$SI and K^{trans}_φ (Table 5). However, the differences between the AUCs for $V_p\_$SI and V_p_φ and for $K^{trans}\_$SI and K^{trans}_φ were not statistically significant ($P = .43$ and $P = .38$ respectively). Using a threshold of $V_p\_\varphi > 1.75$ mL/100 g, sensitivity was 68% and specificity was 88% (PPV = 95%, NPV = 44%) for differentiating grade IV from grade III gliomas.

Within-Subject Reproducibility of V_p and K^{trans} Values by using Magnitude-versus-Phase Techniques

The mean absolute difference between $K^{trans}\_$SI and K^{trans}_φ was 0.06 minutes^{-1} with limits of agreement of ± 0.22 minutes^{-1}, which was statistically different ($P = .001$) (Fig 4*A*). The difference in percentage was 17%, with limits of agreement of $\pm 191\%$. The mean absolute difference between $V_p\_$SI and V_p_φ was 6.7 mL/100 g, with limits of agreement of ± 15.4 mL/100 g, which was statistically different ($P < .0001$) (Fig 4*B*). The difference in percentage was 103% with limits of agreement of $\pm 134\%$. Agreement between $K^{trans}\_$SI and K^{trans}_φ and between $V_p\_$SI and V_p_φ is dependent on the magnitude of measurements, with a good agreement at low values and a poor agreement at high values.

Discussion

Dynamic susceptibility-weighted contrast-enhanced MR perfusion is currently the most frequently used technique to measure CBV in cerebral gliomas, primarily due to the robustness of the technique. Several authors have demonstrated a high degree of correlation between histologic grades and CBV.[1,11] However, CBV measurements from dynamic susceptibility-weighted contrast-enhanced require correction for leakage in areas of blood-brain disruption in tumors and are prone to susceptibility artifacts arising from hemorrhage, calcification, or bone.[12-14]

DCE MR imaging is a T1-weighted technique, which is, as a consequence, less sensitive to susceptibility artifacts. It has been introduced more recently to quantify the absolute plasma volume and the volume transfer coefficient, which measures the degree of contrast leakage from the intravascular to the extravascular compartment. Although there have been numerous studies using

DCE MR perfusion to grade tumors, it is somewhat difficult to compare published values because different research centers have different MR imaging acquisition techniques and postprocessing algorithms. In our study, we compared 2 methods: 1 that assumes that there is linearity between changes in contrast concentration and signal intensity and a more novel approach that uses pre- and postcontrast T1 quantification and a vascular input function derived from MR phase images.

The K^{trans} values obtained by using the magnitude-VIF ($K^{trans}\_$SI) were within the range of those published in 1 of the first studies using DCE MR imaging for grading gliomas by Roberts et al,[11] which used changes in signal intensity to calculate perfusion values.[8] The authors obtained a median transfer constant for grade IV gliomas of 0.107 minutes^{-1}, which is similar to our $K^{trans}\_$SI of 0.15 minutes^{-1}. They also found a statistically significant difference between the transfer constants for grade III and IV gliomas but not between grades II and III, which is consistent with our findings. The median fractional blood volume for grade IV gliomas reported by Roberts et al was only 6%, which (assuming a hematocrit of 0.45) is lower than the 17% value corresponding to our $V_p\_$SI value of 9.4 mL/100 g. They did not find a correlation between fractional blood volume and tumor grade, whereas we found a statistical difference between $V_p\_$SI values for grade III and IV gliomas but not between grade II and III gliomas. Their protocol was slightly different from ours because they had low temporal resolution and used a Patlak analysis, whereas our images were acquired with high temporal resolution and analyzed by deconvolution of the VIF.

A more recent study by Patankar et al[6] used precontrast T1 mapping and a magnitude-derived VIF to demonstrate that CBV can be used to distinguish high-grade and low-grade gliomas. The authors reported CBV values of 1.3%, 3%, and 4% for grade II, III, and IV gliomas, respectively. These results are in the range of our V_p_φ values of 0.64 mL/100 g (CBV = 1.2%), 0.98 mL/100 g (CBV = 1.78%), and 2.16 mL/100 g (CBV = 3.9%) for grade II, III, and IV gliomas, respectively. In contrast to Patankar et al, we did not find a significant difference in V_p_φ between grade II and III gliomas, perhaps due to inaccurate pathologic grading from biopsy. Two patients in our low-grade glioma group had very high perfusion parameters but their gliomas were classified as grade II following biopsy. There was probably a sampling bias because the lesions

Table 5: AUC values for various ROC curves

	AUC for K^{trans}_φ (95% CI)	AUC for K^{trans}_SI (95% CI)	AUC for V_p_φ (95% CI)	AUC for V_p_SI (95% CI)
Low-grade from high-grade gliomas	0.87 (0.73–1)	0.81 (0.59–1)	0.84 (0.69–0.98)	0.84 (0.66–0.91)
Grade III from grade IV gliomas	0.73 (0.46–1)	0.77 (0.54–1)	0.77 (0.58–0.97)	0.84 (0.68–0.99)

enhanced strongly and the patients died shortly after surgery. The other study obtained K^{trans} values of 0.0007 minutes^{-1}, 0.0185 minutes^{-1}, and 0.0250 minutes^{-1} for grade II, III, and IV gliomas, respectively, which are lower than our values and could be due to the use of a different pharmacokinetic model. The authors did not find a statistically significant difference between either grade II and III or grade III and IV gliomas.

In agreement with the published literature, our study showed that V_p and K^{trans} values are dependent on the assumptions made for the conversion of signal intensity to contrast concentration and the choice of vascular input function.[5] Within each subject, there is a bias toward lower values by using the phase method compared with the signal-intensity method. This bias was less important for K^{trans} than for V_p (17% versus 103%), but the limits of agreement are larger (SD of 191% versus 134%). Within each glioma group, the reproducibility of K^{trans}_φ is better than that of K^{trans}_SI. The diagnostic accuracy of K^{trans}_φ was also slightly better (though not statistically significant) than K^{trans}_SI and comparable with conventional MR imaging in our study.

The use of a phase-derived VIF has several advantages over techniques that use a magnitude-derived VIF: Phase does not saturate at high contrast concentration and is less sensitive to inflow effects.[8,9,15] For that reason, some authors have proposed performing 2 injections of 0.05 mmol/kg of gadolinium for DCE MR imaging to minimize the error arising from the conversion of signal intensity to gadolinium concentration from magnitude images.[16] While saturation of signal intensity could lead to an underestimation of the contrast agent concentration, the presence of inflow effects could lead to an overestimation.[17] Our magnitude-VIF based K^{trans} and V_p estimates were higher than those derived from the phase method. This might be due to an underestimation of the contrast agent concentration in the VIF. We obtained lower coefficients of variation for the perfusion values with the phase method. This is expected because phase-derived VIF is less sensitive to inflow effects.[9] Even though 3D gradient-recalled echo sequences are less sensitive to inflow than 2D gradient-recalled echo, perfusion values obtained with the phase method also had lower coefficients of variation than the ones obtained from the SI method. The use of bookend T1 measurements with the phase technique could also have contributed to an improvement in the calculations of perfusion values because this technique can presumably provide more accurate estimation of the gadolinium concentration in tumors.[4]

The disadvantages of using a phase-derived VIF are the following: It requires additional time to process phase images even though they are freely available from the scanner. Measurements can be biased if there is a drift of the phase signal intensity, making estimation of the steady-state baseline less reliable.[18] In certain circumstances, such as when the signal intensity–to-noise-ratio is low, the signal-intensity approach might even yield more useful perfusion measurements because less processing of the data is required than for a phase- or magnitude-based approach, which requires the conversion to gadolinium concentration by using T1 measurements obtained at baseline.[19]

We note 3 potential limitations to our findings: First, the small number of patients with grade II and III gliomas limited our power to detect a statistical difference in the diagnostic accuracy of our novel phase-VIF technique compared with the more conventional magnitude-VIF method. Second, because some patients with grade II gliomas had only a biopsy, a misclassification could have resulted in including these cases. We suspect this surgical sampling bias contributed to the very high coefficients of variation for perfusion parameters in low-grade tumors. Third, there might be a measurement bias due to methodologic differences between the 2D and 3D techniques. However, we do not believe that the different pulse sequences and field strengths had a major systematic effect on pharmacokinetic parameters calculated from phase-derived VIFs with bookend T1 correction. The bookend technique has inherent self-correcting and self-consistency mechanisms that depend little on pulse sequence parameters or field strength. There was not any statistically significant difference in steady-state gadolinium concentrations in tumor between the 2D and 3D acquisitions (data not shown). For the phase-derived VIFs, changes in pulse-sequence parameters and field strength theoretically should not introduce systematic errors either. We found no statistically significant difference in peak gadolinium concentration, area under the first pass, or steady-state gadolinium concentration between the 2D and 3D acquisitions (data not shown). Therefore, it is not clear why there was a near-significant difference in K^{trans}_φ values between the 2D and 3D acquisitions for grade IV gliomas. This is perhaps due to the inherent biologic heterogeneity of these tumors and the subtlety of effects related to the different acquisitions. The similarity of pharmacokinetic parameters between 2D and 3D acquisitions for magnitude-derived VIFs with no T1 correction also suggests that the relationship between signal intensity and gadolinium concentration was consistent and reasonably linear for each of the 2 acquisitions.

Conclusions

We have shown that K^{trans}_φ and V_p_φ values obtained by using the phase-derived VIF with the bookend T1 measurement technique can be used to differentiate low-grade from high-grade gliomas. This novel method can be implemented by using either a 2D or a 3D sequence, but in general, the use of a 3D sequence resulted in better intersubject reproducibility. This approach might improve the diagnostic accuracy of preoperative glioma grading compared with other MR imaging methods currently used to assess tumor perfusion.

Appendix

Kinetic modeling theory was performed by using a 2-compartment extended Tofts model implemented in the nordicICE software (NordicNeuroLab).[20-22] The contrast agent is assumed to be distributed in the plasma volume (V_p) initially with a time-dependent leakage to the extravascular, extracellular space. K^{trans} is the transfer coefficient from the plasma volume to the extravascular, extracellular space, and K_{ep} is the rate constant back to the
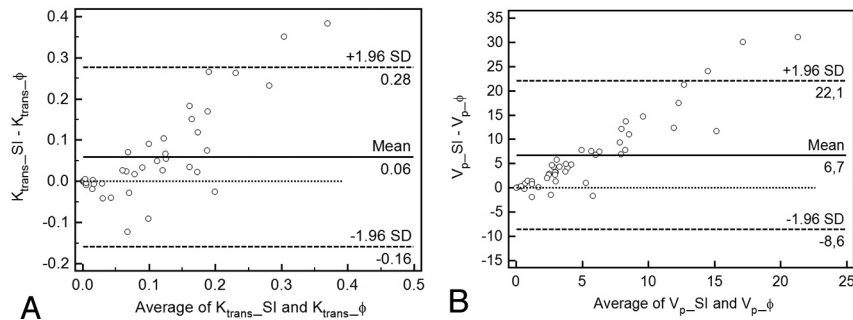
Fig 4. Agreement between K^{trans}_φ and K^{trans}_SI (A), V_p_φ, and V_p_SI (B). A, Bland-Altman plot of difference between K^{trans}_φ and K^{trans}_SI against a mean of K^{trans}_φ and K^{trans}_SI, with a mean absolute difference (bias) (solid line) and 95% confidence interval of the mean difference (limits of agreement) (dashed lines). B, Bland-Altman plot of difference between V_p_φ and $V_p\_SI\_\varphi$ against a mean of V_p_φ and V_p_SI.

plasma space. Given the tissue concentration curve $C_T(t)$ and the vascular input function $C_p(t)$, this equation can be solved by using the following convolution integral:

$$C_T(t) = K^{trans}\int_0^t C_p(\tau)\cdot e^{-K_{ep}(t-\tau)}\,d\tau + V_p\cdot C_p(t).$$

When deconvolution of the VIF is performed, K^{trans} and K_{ep} values are obtained in units of inverse minutes, whereas V_p is a relative fraction.

$C_T(t)$ is not measured directly but is derived from changes in MR signal intensity due to gadolinium injection. For the simpler pharmacokinetic approach by using magnitude images only, we assumed that signal intensity varied linearly with $C_T(t)$. Because this assumption might not be valid at a high concentration of gadolinium, we used the bookend technique for our novel method with a phase-derived VIF. The bookend technique measured T_{1pre} and T_{1post} values, which allowed computation of $C_T(t)$ from changes in signal intensity.

References

1. Law M, Yang S, Wang H, et al. **Glioma grading: sensitivity, specificity, and predictive values of perfusion MR imaging and proton MR spectroscopic imaging compared with conventional MR imaging.** *AJNR Am J Neuroradiol* 2003;24:1989–98
2. Verheul HM, Voest EE, Schlingermann RO. **Are tumours angiogenesis-dependent?** *J Pathol* 2004;202:5–13
3. Ludemann L, Warmuth C, Plotkin M, et al. **Brain tumor perfusion. Comparison of dynamic contrast enhanced magnetic resonance imaging using T1, T2 and T2* contrast, pulsed arterial spin labeling, and H$_2$^{15}O positron emission tomography.** *Eur J Radiol* 2009;70:465–74
4. Brix G, Griebel J, Kiessling F, et al. **Tracer kinetic modelling of tumour angiogenesis based on dynamic contrast-enhanced CT and MRI measurements.** *Eur J Nucl Med Mol Imaging* 2010;37(suppl 1):S30–51
5. Cron GO, Kelcz F, Santyr GE. **Improvement in breast lesion characterization with dynamic contrast-enhanced MRI using pharmacokinetic modeling and bookend T(1) measurements.** *Magn Reson Med* 2004;51:1066–70
6. Patankar TF, Haroon HA, Mills SJ, et al. **Is volume transfer coefficient (Ktrans) related to histologic grade in human gliomas?** *AJNR Am J Neuroradiol* 2005;26:2455–65
7. Donahue KM, Weiskoff RM, Burstein D, et al. **Diffusion and exchange as they influence contrast enhancement.** *J Magn Reson Imaging* 1997;7:102–10
8. Foottit C, Cron GO, Hogan MJ et al. **Determination of the venous output function from MR signal phase: feasibility for quantitative DCE-MRI in human brain.** *Magn Reson Med* 2010;63:772–81
9. Cron GO, Foottit C, Yankeelov TE, et al. **Arterial input functions determined from MR signal magnitude and phase for quantitative DCE-MRI in the human pelvis.** *Magn Reson Med* 2011;66:498–504
10. Weisskoff RM, Zuo CS, Boxerman JL, et al. **Microscopic susceptibility variation and transverse relaxation: theory and experiment.** *Magn Reson Med* 1994;31:601–10
11. Roberts HC, Roberts TPL, Brasch RC, et al. **Quantitative measurement of microvascular permeability in human brain tumors achieved using dynamic contrast-enhanced MR imaging: correlation with histologic grade.** *AJNR Am J Neuroradiol* 2000;21:891–99
12. Calamante F, Vonken E, van Osch MJP. **Contrast agent concentration measurements affecting quantification of bolus-tracking perfusion MRI.** *Magn Reson Med* 2007;58:544–53
13. Mangla R, Kolar B, Zhu T, et al. **Percentage signal recovery derived from MR dynamic susceptibility contrast imaging is useful to differentiate common enhancing malignant lesions of the brain.** *AJNR Am J Neuroradiol* 2011;32:1004–10
14. Hu LS, Baxter LC, Pinnaduwage DS, et al. **Optimized preload leakage-correction methods to improve the diagnostic accuracy of dynamic susceptibility-weighted contrast-enhanced perfusion MR imaging in posttreatment gliomas.** *AJNR Am J Neuroradiol* 2010;31:40–48
15. Kim J, Seethamraju RT, Suh JY, et al. **R1 and R2* changes according to Gd concentration: a potential limiting factor in converting MR signal intensity to Gd concentration.** In: *Proceedings of the 19th Annual Meeting of the International Society for Magnetic Resonance in Medicine*, Montreal, Quebec, Canada; May 6–13, 2011
16. Sourbron S, Ingrisch M, Siefert A, et al. **Quantification of cerebral blood flow, cerebral blood volume and blood-brain-barrier leakage with DCE-MRI.** *Magn Reson Med* 2009;62:205–17
17. Kim YR, Rebro KJ, Schmainda KM. **Water exchange and inflow affect the accuracy of T$_1$-GRE blood volume measurements: implications for the evaluation of tumor angiogenesis.** *Magn Reson Med* 2002;47:1110–20
18. de Bruin PW, Versluis MJ, Yusuf E, et al. **Arterial input functions in dynamic contrast-enhanced MRI: magnitude versus phase.** In: *Proceedings of the 19th Annual Meeting of the International Society for Magnetic Resonance in Medicine*, Montreal, Quebec, Canada; May 6–13, 2011
19. Song HK, Xue Y, Yu J, et al. **Comparison of the standard gadolinium concentration and signal difference methodologies for computation of perfusion parameters in DCE-MRI at various SNRs.** In: *Proceedings of the 19th Annual Meeting of the International Society for Magnetic Resonance in Medicine*, Montreal, Quebec, Canada; May 6–13, 2011
20. Ott RJ, Brada M, Flower MA, et al. **Measurements of blood-brain barrier permeability in patients undergoing radiotherapy and chemotherapy for primary cerebral lymphoma.** *Eur J Cancer* 1991;27:1356–61
21. Tofts PS. **Modeling tracer kinetics in dynamic Gd-DTPA MR imaging.** *J Magn Reson Imaging* 1997;7:91–101
22. Tofts PS, Brix G, Buckley DL, et al. **Estimating kinetic parameters from dynamic contrast-enhanced T(1)-weighted MRI of a diffusable tracer: standardized quantities and symbols.** *J Magn Reson Imaging* 1999;10:223–32